PFC/JA83-10

STIMULATED EMISSION FROM A RELATIVISTIC ELECTRON BEAM IN A VARIABLE PARAMETER LONGITUDINAL MAGNETIC WIGGLER

Wayne A. McMullin, Ronald C. Davidson
and George Johnston

2/83

STIMULATED EMISSION FROM A RELATIVISTIC ELECTRON BEAM IN A VARIABLE PARAMETER LONGITUDINAL MAGNETIC WIGGLER

Wayne A. McMullin, Ronald C. Davidson and George L. Johnston
Plasma Fusion Center
Massachusetts Institute of Technology
Cambridge, Massachusetts 02139

ABSTRACT

The single-particle equations of motion are used to study the stimulated emission from a tenuous relativistic electron beam propagating in the combined solenoidal and variable parameter longitudinal wiggler magnetic fields produced near the axis of a multiple-mirror (undulator) field configuration. The specific case of constant field amplitude and variable wiggler periodicity is studied. It is found that the efficiency of radiation generation can be increased by orders-of-magnitude relative to the case where the wiggler periodicity is constant. This is due to the fact that the phase velocity of the ponderomotive potential in which the electrons are trapped is decreasing, allowing the electrons to exchange energy with the radiation field.

I. INTRODUCTION

In the present article, we investigate free electron laser radiation generation by a tenuous, relativistic electron beam propagating along the axis of a multiple-mirror (undulator) magnetic field in circumstances where the amplitude $B_w(z)$ and wavenumber $k_0(z)$ of the longitudinal wiggler field are allowed to vary slowly with axial position z. The beam radius is assumed to be sufficiently small that the electrons interact only with the axial magnetic field given approximately by Eq. (3). In previous investigations [1–3], radiation generation in such a *longitudinal wiggler* configuration has been studied for the case where the wiggler amplitude and wavenumber are constant. As for the case of a free electron laser with constant-amplitude, constant-wavenumber, *transverse wiggler*, it is found [1–3] that the efficiency of radiation generation is relatively low. However, for a free electron laser with variable parameter transverse wiggler, it has been recently shown [4–8] that the efficiency of radiation generation can be greatly increased relative to that of a constant parameter wiggler. In the present analysis, we extend the techniques developed in Ref. 6 to calculate the efficiency of radiation generation for the case of a variable parameter longitudinal wiggler.

In Sec. II, we outline the basic assumptions and electromagnetic field configuration related to the present analysis. In Sec. III, coupled dynamical equations are derived for the electron energy and slowly varying phase of the ponderomotive bunching force. These equations are analyzed in Sec. IV for the specific case of constant wiggler amplitude $B_w =$ const. and variable wiggler wavenumber $k_0(z)$. By slowly varying the wavenumber $k_0(z)$ of the wiggler magnetic field, the phase velocity of the ponderomotive potential in which the electrons are trapped decreases in the axial direction, thereby allowing the electrons to give up energy to the electromagnetic radiation field. In Sec. V, an analytic expression [Eq.(49)] for the efficiency of radiation generation is derived. It is found that this efficiency can be orders-of-magnitude larger than the efficiency for a constant parameter longitudinal wiggler. Finally, in Sec. V, a numerical example is presented for a radiation source with parameters of interest for electron cyclotron heating of fusion plasmas.

II. ELECTROMAGNETIC FIELD CONFIGURATION AND BASIC ASSUMPTIONS

In the present analysis, we examine the relativistic motion of an electron in the presence of an applied solenoidal and *longitudinal* wiggler magnetic field combined with a circularly polarized, constant-amplitude, transverse electromagnetic wave propagating in the z-direction. The spatial variation of applied field quantities is assumed to be in the z-direction. It is also assumed that the configuration corresponds to a laser oscillator operating at a saturated steady-state amplitude with propagating wave electric field amplitude $\delta E =$ const. and wavenumber $k =$ const. that have negligibly small spatial variation. The density of electrons is assumed to be sufficiently tenuous that $\omega \simeq kc$, and the steady-amplitude electromagnetic wave is specified by

$$\delta E(z,t) = -\delta E[\hat{e}_x \sin(kz - \omega t + \varphi) + \hat{e}_y \cos(kz - \omega t + \varphi)], \tag{1}$$

$$\delta B(z,t) = \left(\frac{ck\delta E}{\omega}\right)[\hat{e}_x \cos(kz - \omega t + \varphi) - \hat{e}_y \sin(kz - \omega t + \varphi)], \tag{2}$$

where φ is an arbitrary phase.

The expression for the applied solenoidal and longitudinal wiggler magnetic field is taken to be of the form[1-3]

$$B(z) = \hat{e}_z\left[B_0 + B_w(z)\sin\int_0^z dz' k_0(z')\right] \tag{3}$$

where $B_0 =$ const. The expression given in Eq.(3) is valid near the axis of the multiple-mirror (undulator) magnetic field, i.e., for $|k_0 r| \ll 1$ where r is the radial distance from the axis of symmetry, and the wiggler amplitude $B_w(z)$ and wavenumber $k_0(z)$ are allowed to vary slowly as a function of axial coordinate z over a distance k_0^{-1}. In what follows it is assumed that the field amplitudes are ordered by

$$|B_0| \gg |B_w| \gg |\delta E|. \tag{4}$$

Before entering the interaction region, the electrons have an initial axial momentum p_{z0}, an initial transverse momentum $p_{\perp 0}$, and energy $E_0 = (c^2p_{z0}^2 + c^2p_{\perp 0}^2 + m^2c^4)^{\frac{1}{2}} = \gamma_0 mc^2$, where $\gamma_0^2 = (1 - v_{\perp 0}^2/c^2 - v_{z0}^2/c^2)^{-1}$. As for the case of an electron cyclotron maser, it is necessary that the electrons enter the interaction region with an initial transverse momentum, because it is the excess transverse momentum that drives the instability and causes radiation amplification.

III. EQUATIONS OF MOTION

In this section, we make use of the relativistic Lorentz force equation for an electron moving in the combined electromagnetic fields given by Eqs.(1)-(3) to determine coupled equations for the electron energy and phase of the ponderomotive bunching force. The equations of motion can be expressed as (where $\omega \simeq kc$)

$$\frac{dp_x}{dt} = -e\frac{v_y}{c}\left[B_0 + B_w(z)\sin\int_0^z dz'k_0\right] + e\delta E(1 - kv_z/\omega)\sin(kz - \omega t + \varphi), \tag{5}$$

$$\frac{dp_y}{dt} = e\frac{v_x}{c}\left[B_0 + B_w(z)\sin\int_0^z dz'k_0\right] + e\delta E(1 - kv_z/\omega)\cos(kz - \omega t + \varphi), \tag{6}$$

$$\frac{dp_z}{dt} = \frac{e}{c}\delta E[v_x \sin(kz - \omega t + \varphi) + v_y \cos(kz - \omega t + \varphi)], \tag{7}$$

$$\frac{dE}{dt} = e\delta E[v_x \sin(kz - \omega t + \varphi) + v_y \cos(kz - \omega t + \varphi)]. \tag{8}$$

Multiplying Eq.(7) by c and subtracting the resulting equation from Eq.(8) yields the constant of the motion

$$E - cp_z = E_0 - cp_{z0} = \text{const.}, \tag{9}$$

which relates the axial momentum p_z to the energy E. Defining the relative change in energy by

$$W \equiv 1 - E/E_0 = 1 - \gamma/\gamma_0, \tag{10}$$

and making use of Eq.(9), gives an expression for the axial momentum in terms of W,

$$p_z = p_{z0}[1 - cW/v_{z0}]. \tag{11}$$

Defining $p_+ = p_x + ip_y$, and combining Eqs.(5) and (6) give

$$\frac{d}{dt}\left\{p_+ \exp\left[-i\int_0^t dt\left(eB_0 + eB_w \sin\int_0^z dz'k_0\right)c/E\right]\right\} =$$
$$ie\delta E(1 - v_z/c)\exp\left[-i(kz - \omega t + \varphi) - i\int_0^t dt\left(eB_0 + eB_w \sin\int_0^z dz'k_0\right)c/E\right]. \quad (12)$$

To evaluate the integrals appearing in the exponential, we define

$$\int_0^t dt eB_0/mc\gamma = \omega_b\int_0^t dt/\gamma = \omega_b\varsigma, \quad (13)$$

and assume

$$\left|\frac{B_w}{k_0 p_z}\right| \gg \left|\frac{1}{k_0}\frac{d}{dz}\left(\frac{B_w}{k_0 p_z}\right)\right|.$$

The second integral in the exponential in Eq.(12) is approximately

$$\int_0^t \frac{dt}{E} ecB_w \sin\int_0^z dz'k_0 = -\int_0^z \frac{dz}{p_z}\frac{eB_w}{ck_0}\frac{d}{dz}\cos\int_0^z dz'k_0$$
$$\simeq \frac{-eB_w}{ck_0 p_z}\left[\cos\int_0^z dz'k_0 - 1\right]. \quad (14)$$

It is further assumed that the inequality,

$$|p_{\perp 0}| \gg \Bigg| e\delta E\int_0^t dt(1 - v_z/c)$$
$$\times \exp\left[-i(kz - \omega t + \varphi) - i\omega_b\varsigma + ieB_w\left(\cos\int_0^z dz'k_0 - 1\right)/k_0 p_z c\right]\Bigg|,$$

is satisfied, so that the solution to Eq.(12) can be approximated by

$$p_+ \simeq p_{\perp 0} \quad \exp i\left[\varphi_0 + \omega_b\varsigma - eB_w\left(\cos\int_0^z dz'k_0 - 1\right)/k_0 p_z c\right]. \quad (15)$$

Therefore, the magnitude of the transverse electron momentum remains approximately equal to the initial value $p_{\perp 0}$, although the individual x and y components of the momentum are strongly modulated by the longitudinal wiggler field.

Choosing the independent variable to be the z-coordinate, Eq.(8) can be expressed in terms of p_+ as

$$\frac{dE}{dz} = \frac{ie\delta E}{2p_z}[p_+^* \exp i(\omega t - kz - \varphi) - p_+ \exp i(kz - \omega t + \varphi)]. \tag{16}$$

Substituting Eq.(15) into Eq.(16), expanding the sinusoidally varying argument of the exponentials in a series of ordinary Bessel functions $J_\ell(a)$, and defining the slowly varying phase of the ponderomotive bunching force by ($\ell = 1, 2, 3, ...$)

$$\psi = kz - \omega t + \omega_b\varsigma + \ell \int_0^z dz' k_0 + eB_w/ck_0p_z + \varphi + \varphi_0 - \ell\pi/2, \tag{17}$$

we find that Eq.(16) can be expressed as

$$\frac{dW}{dz} = \frac{-e\delta E}{E_0}\frac{p_{\perp 0}}{p_{z0}}\frac{J_{-\ell}[eB_w/ck_0p_{z0}(1 - cW/v_{z0})]}{(1 - cW/v_{z0})}\sin\psi. \tag{18}$$

In obtaining Eq.(18), use has been made of Eqs.(10) and (11), and only the term with the slowly varying phase ψ has been retained. Differentiating Eq.(17) with respect to z, and making use of Eqs.(10) and (11) yields ($\omega_{c0} = eB_0/mc\gamma_0$)

$$\frac{d\psi}{dz} = (k + \ell k_0) - \frac{\omega(1 - W) - \omega_{c0}}{v_{z0}(1 - cW/v_{z0})} + \frac{d}{dz}\left[\frac{eB_w}{ck_0p_{z0}(1 - cW/v_{z0})}\right]. \tag{19}$$

Eqs.(18) and (19) constitute the desired dynamical equations for the phase of the ponderomotive bunching force and the electron energy. Here, the radiation emission occurs at the ℓ'th harmonic of the wiggler wavenumber. In order to obtain an approximate solution to these equations, in Sec. IV we expand about the synchronous energy and phase for which ψ is constant.

IV. MOTION ABOUT THE SYNCHRONOUS ENERGY AND PHASE

In this section the synchronous relative energy W_r and phase ψ_r are defined, and the resulting equations are used to determine the functional dependence of the wiggler amplitude B_w and wavenumber k_0 upon the z-coordinate. For present purposes, we will take B_w to be constant and only consider variable $k_0(z)$. Equations (18) and (19) are then expanded about W_r to determine the conditions for the electron energy to remain close to the synchronous value.

The synchronous phase ψ_r is defined as the value of ψ for which Eq.(19) vanishes,

$$\begin{aligned}\frac{d\psi_r}{dz} &= (k + \ell k_0) - \frac{\omega(1 - W_r) - \omega_{c0}}{v_{z0}(1 - cW_r/v_{z0})} + \frac{d}{dz}\left[\frac{eB_w}{ck_0 p_{z0}(1 - cW_r/v_{z0})}\right] \\ &= 0,\end{aligned} \tag{20}$$

where $W_r \equiv 1 - \gamma_r/\gamma_0$. In the following, the quantity $eB_w/ck_0p_{z0}(1 - cW_r/v_{z0})$ is assumed to be constant, so that Eq.(20) yields

$$(1 - cW_r/v_{z0})\ell k_0 v_{z0} = \omega(1 - v_{z0}/c) - \omega_{c0}. \tag{21}$$

Since $\omega =$ const. is assumed, Eq.(21) gives the constraint that $k_0(1 - cW_r/v_{z0})$ must be independent of z.

From Eq.(18), the resonant relative energy W_r is found to satisfy

$$\begin{aligned}\frac{dW_r}{dz} &= \frac{-e\delta E}{E_0}\frac{p_{\perp 0}}{p_{z0}}\frac{J_{-\ell}[eB_w/ck_0p_{z0}(1 - cW_r/v_{z0})]}{(1 - cW_r/v_{z0})}\sin\psi_r \\ &\equiv -\frac{\Delta \sin\psi_r}{(1 - cW_r/v_{z0})}.\end{aligned} \tag{22}$$

Rewriting Eq.(22) as

$$\frac{d(1 - cW_r/v_{z0})^2}{dz} = \frac{2c\Delta}{v_{z0}}\sin\psi_r, \tag{23}$$

we see from Eqs.(21) and (23) that k_0^{-2} exhibits a linear dependence on the axial coordinate z. In terms of the wiggler wavelength $\lambda_0(z) = 2\pi/k_0(z)$, we find

$$\lambda_0^2(z) = [\lambda_0^2(L) - \lambda_0^2(0)]z/L + \lambda_0^2(0), \tag{24}$$

where L is the length of the interaction region. From Eq.(21) it is evident that $\lambda_0(0)$ and $\lambda_0(L)$ are related by

$$[1 - cW_r(L)/v_{z0}]\lambda_0(0) = \lambda_0(L). \tag{25}$$

Solving Eq.(23), and substituting into Eq.(25) provides the further relation

$$\lambda_0^2(L) = [1 + \sin\psi_r 2cL\Delta/v_{z0}]\lambda_0^2(0), \tag{26}$$

and Eq.(24) can be expressed as

$$\lambda_0^2(z) = \lambda_0^2(0)[1 + \sin\psi_r 2cz\Delta/v_{z0}]. \tag{27}$$

In order for the electrons to give up energy to the electromagnetic radiation field, they must be decelerating, which from Eq.(22) imposes the requirement

$$\Delta \sin\psi_r < 0. \tag{28}$$

From the condition in Eq.(28), we find from Eq.(27) that the longitudinal wiggler wavelength *decreases* as the axial coordinate z is increased, with the result that the ponderomotive potential wells slow down as they pass through the wiggler magnetic field. This allows the electrons to transfer energy to the electromagnetic radiation field.

In order for the electrons to remain close to the synchronous values (W_r, ψ_r), the electron motion must exhibit stable oscillations about the synchronous values for small-amplitude perturbations. To study this small-amplitude motion, the quantity W is expanded,

$$W = W_r + \delta W = W_r - \delta\gamma/\gamma_0, \tag{29}$$

with the assumption that $|W_r| \gg |\delta W|, |\delta\gamma/\gamma_0|$. We substitute Eq.(29) into Eqs.(18) and (19), linearize the resulting equations for small δW, and assume that the following inequalities are satisfied

$$|\ell k_0(z)| \gg \left| a \frac{d \ln k_0(z)}{dz} \right|,$$

$$|\ell k_0(z)| \gg \left| a \frac{d \ln \delta W}{dz} \right|,$$

$$|\ell k_0(z)| \gg \left| a \frac{k_0^2(z)}{k_0^2(0)} \Delta \frac{\sin \psi}{\beta_{z0}} \left[1 + \frac{a}{J_{-\ell}(a)} \frac{dJ_{-\ell}(a)}{da} \right] \right|,$$

$$|\sin \psi - \sin \psi_r| \gg \left| \frac{\delta W \sin \psi}{\beta_{z0}} \frac{k_o(z)}{k_0(0)} \left[1 + \frac{a}{J_{-\ell}(a)} \frac{dJ_{-\ell}(a)}{da} \right] \right|, \tag{30}$$

where $a = eB_w/ck_0(z)p_z$, $\beta_{z0} = v_{z0}/c$, and $\Delta = (e\delta E/E_0)(\beta_{\perp 0}/\beta_{z0})J_{-\ell}(a)$. This gives the approximate dynamical equations

$$\frac{d\delta\gamma}{dz} = \gamma_0 \Delta \frac{k_0(z)}{k_0(0)} (\sin \psi - \sin \psi_r), \tag{31}$$

$$\frac{d\psi}{dz} = \frac{\ell k_0^2(z)}{\beta_{z0} k_0(0)} \frac{\delta\gamma}{\gamma_0}. \tag{32}$$

The conditions in Eqs.(30) for Eqs.(31) and (32) to be valid are essentially conditions that the spatial variation be slow over a wiggler wavelength. Equations (31) and (32) can also be derived from the Hamiltonian H defined by

$$H = \frac{\gamma_0 \ell k_0^2(z)}{2\beta_{z0} k_0(0)} \left(\frac{\delta\gamma}{\gamma_0} \right)^2 + \gamma_0 \Delta \frac{k_0(z)}{k_0(0)} (\cos \psi + \psi \sin \psi_r), \tag{33}$$

where $d\psi/dz = \partial H/\partial\delta\gamma$ and $d\delta\gamma/dz = -\partial H/\partial\psi$. Here $\delta\gamma$ plays the role of the canonical momentum coordinate and ψ plays the role of the position coordinate. The Hamiltonian given by Eq.(33) is of the same functional form as that for a free electron laser utilizing a transverse helical wiggler and studied extensively by Kroll, Morton, and Rosenbluth[6]. The Hamiltonian has the form of a nonrelativistic single particle Hamiltonian with an effective "mass" that is a function of the z-coordinate and a potential function U that is also z-dependent

$$U = \gamma_0 \Delta \frac{k_0(z)}{k_0(0)} (\cos \psi + \psi \sin \psi_r). \tag{34}$$

Here, it is assumed that a value of ψ_r exists such that

$$\left|\frac{dW_r}{dz}\right| < \left|\frac{\Delta}{1 - W_r/\beta_{z0}}\right|$$

and $\Delta \sin\psi_r < 0$. Taking $\Delta < 0$ and $\sin\psi_r > 0$, the potential function U consists of a series of decreasing-amplitude troughs in which the electrons become trapped, with successive minima located at $\psi = \psi_r + 2\pi n$ and maxima located at $\psi = \pi - \psi_r + 2\pi n$, provided ψ_r lies in the range $0 < \psi_r < \pi/2$. For the case where $\Delta > 0$ and $\sin\psi_r < 0$, the range of values of ψ_r is restricted to the interval $-\pi/2 < \psi_r < 0$. In the following analysis, for the sake of definiteness, it is assumed that ψ_r lies in the interval $0 < \psi_r < \pi/2$. Also, since the trajectories of the electrons in the phase space $(\psi, \delta\gamma)$ have 2π-periodicity in ψ, the analysis is restricted to values of ψ in the range of $-\pi < \psi < \pi$.

The maximum value of the Hamiltonian H occurs for $\psi = \pi - \psi_r, \delta\gamma = 0$ and is given by $(\Delta < 0)$

$$H_{max} = -\gamma_0 \Delta \frac{k_0(z)}{k_0(0)} [\cos\psi_r - (\pi - \psi_r)\sin\psi_r]. \tag{35}$$

The electrons remain trapped in the potential wells for $|\delta\gamma| < |\delta\gamma_{max}|$, where $\delta\gamma_{max} = \delta\gamma(\psi = \psi_r)$. Making use of Eq.(35) in Eq.(33) gives

$$|\delta\gamma| < |\delta\gamma_{max}| = \left[\frac{-4\beta_{z0}\gamma_0^2\Delta}{\ell k_0(z)} [\cos\psi_r - (\pi/2 - \psi_r)\sin\psi_r]\right]^{\frac{1}{2}}. \tag{36}$$

The maximum closed contour in the phase space (γ, ψ) for which the electrons remain trapped in the potential (and are also decelerating) is illustrated in Fig. 1, where ψ_2 is defined by

$$\psi_2 = \pi - \psi_r, \tag{37}$$

and ψ_1 and ψ_2 are related by

$$\cos\psi_1 + \psi_1 \sin\psi_r = \cos\psi_2 + \psi_2 \sin\psi_r. \tag{38}$$

The quantities ψ_1 and ψ_2 are the turning points of Eq.(33), and are plotted as a function of ψ_r in Fig. 2.

The electrons remain trapped in the potential wells with energy close to the resonant value γ_r provided that the area of the closed contour in phase space,

$$A = \oint \delta\gamma d\psi, \tag{39}$$

remains approximately constant. The area enclosed in the outermost phase space contour illustrated in Fig. 1 is determined from Eqs.(35), (33), and (39). This gives (for $\Delta < 0$)

$$A = \left(\frac{-2\beta_{z0}\gamma_0^2\Delta}{\ell k_0(z)}\right)^{\frac{1}{2}} \int_{\psi_1}^{\psi_2} d\psi[\cos\psi + \cos\psi_r - (\pi - \psi_r - \psi)\sin\psi_r]$$
$$= 8\left(\frac{-\beta_{z0}\gamma_0^2\Delta}{\ell k_0(z)}\right)^{\frac{1}{2}}\Gamma(\psi_r), \tag{40}$$

where the quantity $\Gamma(\psi_r)$ is plotted versus ψ_r in Fig.3. With $k_0(z)$ specified by Eq.(27), it is evident that the first condition in Eq.(30) assures that the variation of A over a wiggler wavelength remains small so that the motion of the electrons about the synchronous energy may be regarded as adiabatic.

Finally, we note that several approximations have been made in order for the preceding analysis to hold. In retaining only the axial magnetic field component [Eq.(3)], it has been assumed that the effects of the lowest-order *radial* magnetic field, [3]

$$B_r \simeq -\frac{1}{2}B_w k_0(z) r \cos\int_0^z dz' k_0(z'), \tag{41}$$

on the electron motion and ponderomotive force bunching phase ψ are negligibly small. Assuming that the first inequality in Eq.(30) is satisfied, it can be shown that the effect of B_r on the constraint equation (9) is negligibly small provided the inequality [3]

$$(1-\beta_{z0}) \gg \left|\frac{B_w}{B_0}\frac{k_0(z)}{k_0(0)}\frac{\beta_{\perp 0}^2}{\beta_{z0}}\sum_{\ell=-\infty}^{\infty}\sum_{n=-\infty}^{\infty}\frac{J_\ell(a)J_n(a)}{(1+\ell k_0 v_{z0}\gamma_0/\omega_b)(1+nk_0 v_{z0}\gamma_0/\omega_b)}\right| \tag{42}$$

is satisfied. Here, it is assumed that system parameters are removed from resonance so that the denominators in Eq.(42) do not vanish. Also, the effects of B_r on the bunching force phase ψ are small whenever [3]

$$1 \gg \frac{\omega_b}{k_0 v_{z0}\gamma_0}\frac{k}{2k_0}\left(\frac{\beta_{\perp 0}}{\beta_{z0}}\right)^2\left|\sum_{n=-\infty}^{\infty}\frac{J_n^2(a)}{(n+\omega_b/k_0 v_{z0}\gamma_0)^2}\right|. \tag{43}$$

For Eq.(15) to hold, it can be shown that the inequality

$$|\beta_{\perp 0}| \gg |e\delta E(1-\beta_{z0})J_{-\ell}(a)/cp_{z0}|\left|\int_0^z dz k_0(z)\exp(i\psi)/k_0(0)\right| \tag{44}$$

must be satisfied, where use has been made of Eq.(9), and only the term with the slowly varying ponderomotive phase defined in Eq.(17) has been retained. To estimate the integral appearing in the above inequality, we make use of Eq.(27) for $k_0(z)$ and $\psi \simeq \psi_r =$ const. This gives, for Eq.(44),

$$\beta^2_{\perp 0} \gg \left|\frac{(1-\beta_{z0})\beta_{zo}}{\sin\psi_r}\right|\left|1-\sqrt{1+\frac{2z\Delta}{\beta_{z0}}\sin\psi_r}\right|. \quad (45)$$

In Sec. V, it will be shown that Eq.(45) places a stringent limitation on the efficiency of radiation generation.

V. EFFICIENCY OF RADIATION GENERATION

In this section, the efficiency of radiation generation is determined for the electrons that are trapped in the decelerating ponderomotive potential. The efficiency of radiation generation for variable wiggler wavenumber $k_0(z)$ is compared to the efficiency for a constant parameter longitudinal wiggler with $k_0 = \text{const}$. Also, the conditions under which the electrons do not detrap within the interaction region are determined. Finally, a numerical example is presented.

The electrons entering the interaction region are assumed to enter at an arbitrary initial phase ψ_0. As illustrated in Fig. 1, electrons with energy $\gamma_r mc^2$ are trapped in the potential well only for

$$\psi_1 < \psi_0 < \psi_2, \tag{46}$$

where ψ_1 and ψ_2 are defined in Eqs.(38) and (37). It is also assumed that the electrons enter with initial energy $\gamma_r mc^2$ and $\delta\gamma = 0$ so that the fraction of electrons trapped in the potential wells is given by

$$f_T = (\psi_2 - \psi_1)/2\pi. \tag{47}$$

The quantity f_T is plotted as a function of ψ_r in Fig. 4. The trapped electron efficiency is given by

$$\eta_T = \frac{\gamma_0 W_r(L)}{(\gamma_0 - 1)}, \tag{48}$$

where $W_r(L)$ is obtained from Eqs.(25) and (26), and L is the length of the interaction region. Expressed in terms of the wiggler wavenumber, the quantity η_T is given by ($\Delta \sin\psi_r < 0$)

$$\begin{aligned}\eta_T &= \frac{\gamma_0\beta_{z0}}{(\gamma_0 - 1)}\left[1 - \left(1 + \frac{2L\Delta}{\beta_{z0}}\sin\psi_r\right)^{\frac{1}{2}}\right] \\ &= \frac{\gamma_0\beta_{z0}}{(\gamma_0 - 1)}\left[1 - \frac{k_0(0)}{k_0(L)}\right],\end{aligned} \tag{49}$$

where Eqs.(25) and (26) have been substituted into Eq.(48). The total "ideal" efficiency of radiation generation is then equal to the product of the trapped electron fraction f_T and the efficiency η_T,

$$\eta_V = f_T \eta_T. \tag{50}$$

Although it is desirable that η_T be close to the (maximum) value of unity, it is evident that the inequality in Eq.(45) imposes a stringent limitation on η_T, i.e.,

$$\left|\beta_{\perp 0}^2 \sin\psi_r\right| \gg |(1-\beta_{z0})(\gamma_0-1)\eta_T/\gamma_0|. \tag{51}$$

For $0 > 2L\Delta/\beta_{z0} \geq -1$, the quantity $(\gamma_0 - 1)\eta_V/\gamma_0\beta_{z0}$ achieves its maximum value when $\psi_r \simeq 40°$. When $2L\Delta/\beta_{z0} < -1$, the quantity $(\gamma_0 - 1)\eta_V/\gamma_0\beta_{z0}$ achieves its maximum value for $\psi_r < 40°$, under the restriction that the argument of the square root appearing in Eq.(49) does not become negative.

For the case of constant wiggler wavenumber, $k_0 =$ const., the efficiency of radiation generation is given approximately by [6]

$$\eta_c = \frac{2\pi\beta_{z0}}{\ell L k_0(0)}\frac{\gamma_0}{(\gamma_0-1)}. \tag{52}$$

Comparing this result to Eq.(50) gives

$$\frac{\eta_V}{\eta_c} = \frac{\ell L k_0(0) f_T}{2\pi}\left[1-\frac{k_0(0)}{k_0(L)}\right]. \tag{53}$$

Typically, the quantity $Lk_0(0)$ is sufficiently large that η_c is less than a few per cent. From Eq. (53), it is evident that, by varying the wiggler wavenumber $k_0(z)$, the efficiency of radiation generation can be increased by orders-of-magnitude relative to the efficiency for constant wiggler wavenumber, provided $f_T[1 - k_0(0)/k_0(L)]$ does not become vanishingly small.

The expressions given by Eqs.(47), (49), and (50) are valid provided the electrons remain trapped in the ponderomotive potential within the interaction region. Conditions for the electrons to remain trapped can be determined from the (slowly changing) area inside the closed phase-space contour given in Eq.(39). It is assumed that the electrons enter the interaction region with $\delta\gamma = 0$ and $\psi = \psi_0$. Solving Eq.(33) for $\delta\gamma$ that appears in Eq.(39), we find

$$A = 8\left(\frac{-\beta_{z0}\gamma_0^2\Delta}{\ell k_0(0)}\right)^{\frac{1}{2}}\overline{\Gamma}(\psi_r,\psi_0), \tag{54}$$

with

$$\overline{\Gamma}(\psi_r,\psi_0) = \frac{\sqrt{2}}{8}\int_{\overline{\psi_1}}^{\overline{\psi_2}} [\cos\psi + \psi\sin\psi_r - \cos\psi_0 - \psi_0\sin\psi_r]^{\frac{1}{2}}. \tag{55}$$

Here, $\overline{\psi_1}$ and $\overline{\psi_2}$ are illustrated in Fig. 1. Because $\psi_1 < \overline{\psi_1} < \psi_r$ and $\psi_r < \overline{\psi_2} < \psi_2$, then either $\overline{\psi_1} = \psi_0$ or $\overline{\psi_2} = \psi_0$ must be satisfied, depending on the interval in which ψ_0 is located. The other limit in Eq.(55) is then determined by a relation analogous to Eq.(38). The maximum phase-space area at any z is given by Eq.(40). Equating Eqs.(54) and(40) then determines the value $z = z_u$ at which the electrons become untrapped

$$\frac{k_0(0)}{k_0(z_u)} = \frac{\overline{\Gamma}^2(\psi_r, \psi_0)}{\Gamma^2(\psi_r)}. \tag{56}$$

Making use of Eq.(27) in Eq.(56) and solving for z_u gives

$$z_u = \frac{\overline{\Gamma}^4/\Gamma^4 - 1}{2 \sin \psi_r \Delta/\beta_{z0}} = \frac{L(1 - \overline{\Gamma}^4/\Gamma^4)}{1 - [1 - (\gamma_0 - 1)\eta_T/\gamma_0\beta_{z0}]^2}, \tag{57}$$

where Eq.(49) has been substituted. As long as $z_u > L$ the electrons remain trapped throughout the interaction region. The condition $z_u > L$ can be expressed as

$$1 < \frac{(1 - \overline{\Gamma}^4/\Gamma^4)}{1 - [1 - (\gamma_0 - 1)\eta_T/\gamma_0\beta_{z0}]^2} = \frac{(1 - \overline{\Gamma}^4/\Gamma^4)}{1 - k_0^2(0)/k_0^2(L)}. \tag{58}$$

Provided $\overline{\Gamma}^4/\Gamma^4$ does not approach close to unity, this condition is readily satisfied. The quantity $\overline{\Gamma}^4(\psi_r, \psi_0)/\Gamma^4(\psi_r)$ is plotted versus ψ_0 for several values of ψ_r in Fig. 5. From Fig. 5, for $0° \leq \psi_r \leq 40°$, it is evident that the quantity $\overline{\Gamma}^4/\Gamma^4$ remains close to zero whenever $0° \leq \psi_0 \leq 90°$.

As a numerical example, we choose parameters for a radiation source that would be of interest for electron cyclotron heating of fusion plasmas. It is assumed that the resonator has no losses so that the power radiated is determined by the energy balance equation

$$P = (\gamma_0 - 1)(mc^2/e)I\eta_V, \tag{59}$$

where I is the electron beam current. For the electron beam, we also choose $\gamma_0 = 2$, $\beta_{\perp 0} = 0.25$, and $\beta_{z0} = 0.81$, corresponding to an electron energy of 1 Mev. The assumed magnetic field parameters are $B_0 = 10$ kG, wiggler field amplitude $B_w = 3$kG, and wiggler wavenumber $k_0(0) = 5.77\text{cm}^{-1}$. The output frequency at the fundamental harmonic ($\ell = 1$) is then $f = 210$ GHz. The interaction length is taken to be $L = 219$ cm, as well as $2L\Delta/\beta_{z0} = -0.5$, $\psi_r = 40°$, and $\delta E = 600$ statvolt cm^{-1}. These parameters then give for the variable wiggler wavelength $\lambda_0(z) = \lambda_0(0)[1 - 0.321z/L]^{\frac{1}{2}}$ and $\lambda_0(L)/\lambda_0(0) = 0.82$. The trapped electron efficiency is found to be $\eta_T = 29\%$, which gives for the total "ideal" efficiency $\eta_V = 12\%$. If we also assume an electron beam with current $I = 16.7$ Amperes and beam radius $R_b = 1$ mm, then from Eq.(59), the radiated power is $P = 1$ MW.

VI. CONCLUSIONS

We have examined the efficiency of radiation generation by a relativistic electron beam propagating along the axis of a multiple-mirror (undulator) magnetic field approximated by Eq.(3). The specific case studied corresponds to constant wiggler amplitude with wiggler wavenumber varying axially according to Eq.(27). The efficiency is improved by orders-of-magnitude relative to the case where the wiggler wavenumber is constant. Since the improved efficiency relies on trapped electrons in the decelerating ponderomotive potential, fairly substantial electromagnetic field amplitudes are required. This mechanism of radiation generation appears to be ideally suited for the power levels and electron cyclotron frequency ranges necessary to heat fusion plasmas. The undulator (multiple-mirror) magnetic field configuration is more easily constructed and its periodicity more easily varied than the transverse wiggler field use in a standard free electron laser. Also, the longitudinal wiggler field configuration produces a higher output frequency for a given electron energy than does a transverse wiggler field provided $\gamma_0^2\beta_{\perp 0}^2 \leq 1$. Moreover, the longitudinal wiggler configuration provides a much higher output frequency than an electron cyclotron maser (gyrotron) at the same average value of axial magnetic field.

REFERENCES

1. W.A. McMullin and G. Bekefi, Phys. Rev. A *25*, 1826 (1982).
2. R.C. Davidson and W.A. McMullin, Phys. Rev. A *26*, 1997 (1982).
3. R.C. Davidson and W.A. McMullin, Phys. Fluids *26*,in press (1983).
4. C.A. Brau, IEEE J. Quant. Electron. *QE-16*, 335 (1980).
5. P. Sprangle, C.M. Tang, and W.M. Manheimer, Phys. Rev. A *21*, 302 (1980).
6. N.M. Kroll, P.L. Morton, and M.N. Rosenbluth, IEEE J. Quant. Electron. *QE-17*, 1436 (1981).
7. D. Prosnitz, A. Szoke, and V.K. Neil, Phys. Rev. A *24*, 1436 (1981).
8. "Free Electron Generators of Coherent Radiation," Physics of Quantum Electronics, Vol. 7, edited by S.F. Jacobs, H.S. Pilloff, M. Sargent III, M.O. Scully, and R. Spitzer (Addison-Wesley, Reading, Mass., 1980).

FIGURE CAPTIONS

Fig.1 Closed phase space orbits.

Fig.2 Plot of ψ_1, ψ_2 versus the synchronous phase ψ_r.

Fig.3 Plot of the phase space area function $\Gamma(\psi_r)$ versus $\sin\psi_r$.

Fig.4 Plot of the fraction of trapped electrons versus ψ_r.

Fig.5 Plot of the detrapping function $\overline{\Gamma}^4(\psi_r, \psi_0)/\Gamma^4(\psi_r)$ versus the initial phase ψ_0 for various values of ψ_r.

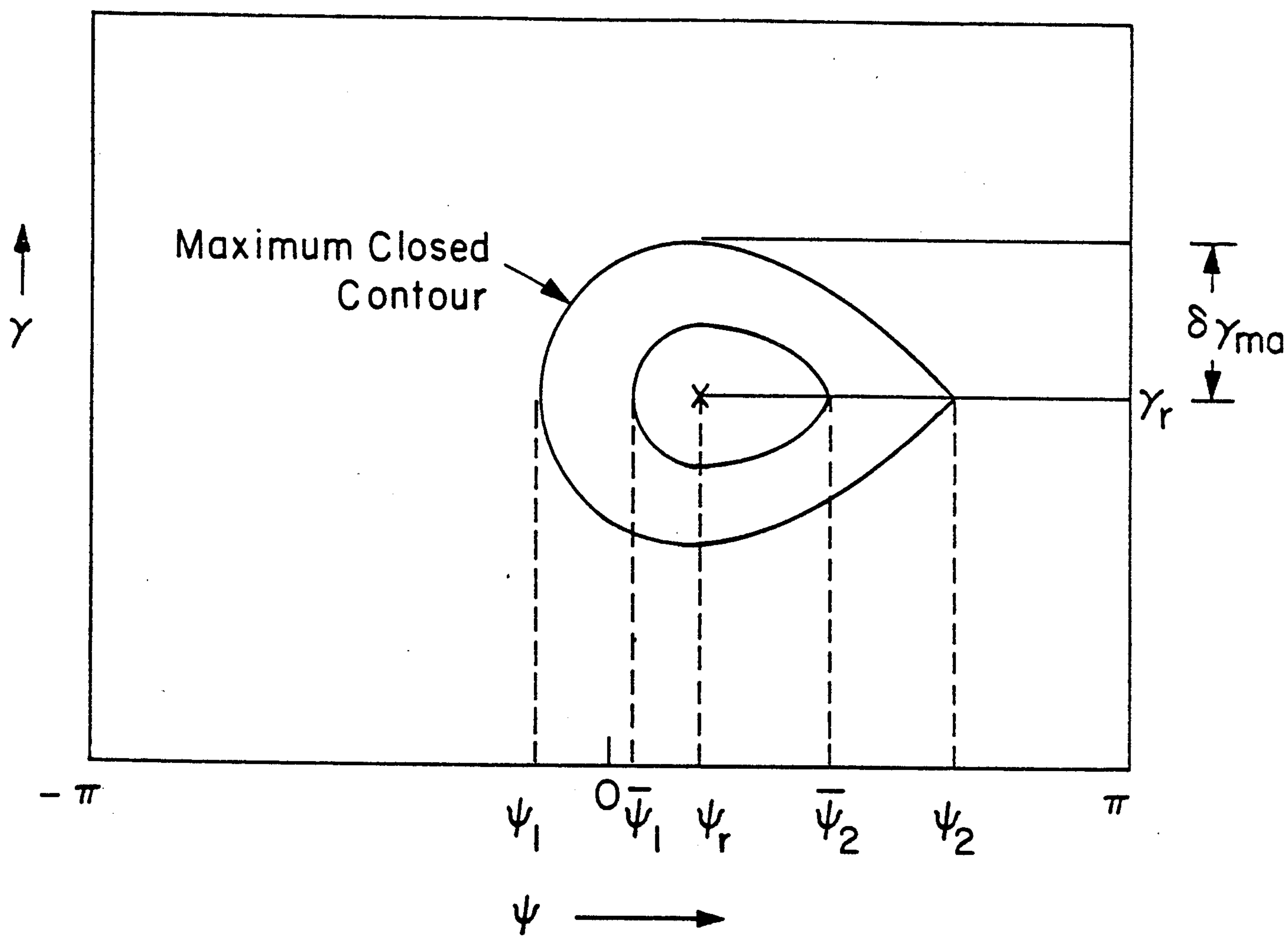
Maximum Closed
Contour
γ
$\delta\gamma_{ma}$
γ_r
$-\pi$
ψ_1
O
$\bar{\psi}_1$
ψ_r
$\bar{\psi}_2$
ψ_2
π
ψ

Fig. 1

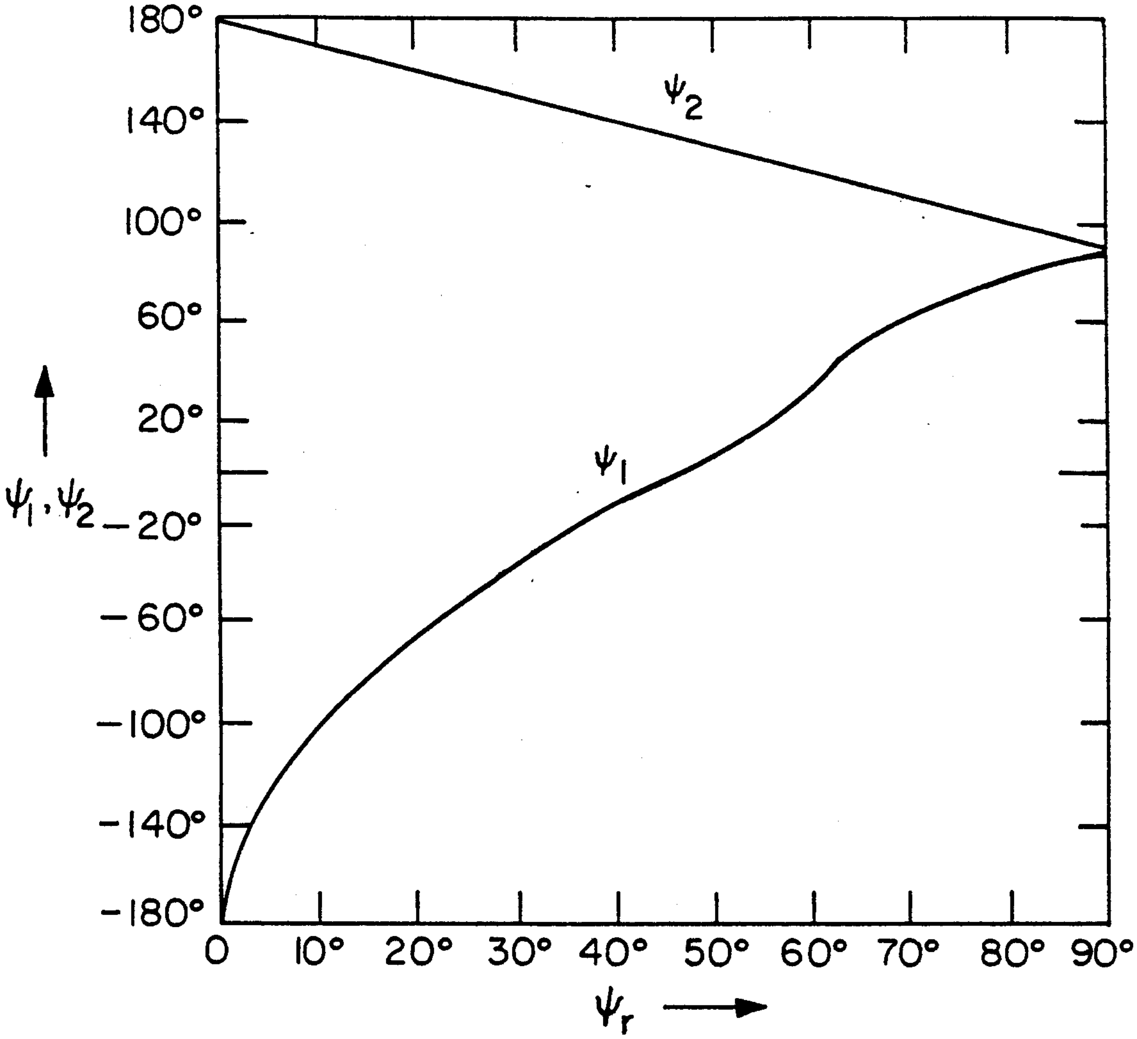
180°
140°
100°
60°
20°
-20°
-60°
-100°
-140°
-180°
ψ_1, ψ_2
ψ_2
ψ_1
0
10°
20°
30°
40°
50°
60°
70°
80°
90°
ψ_r

Fig. 2

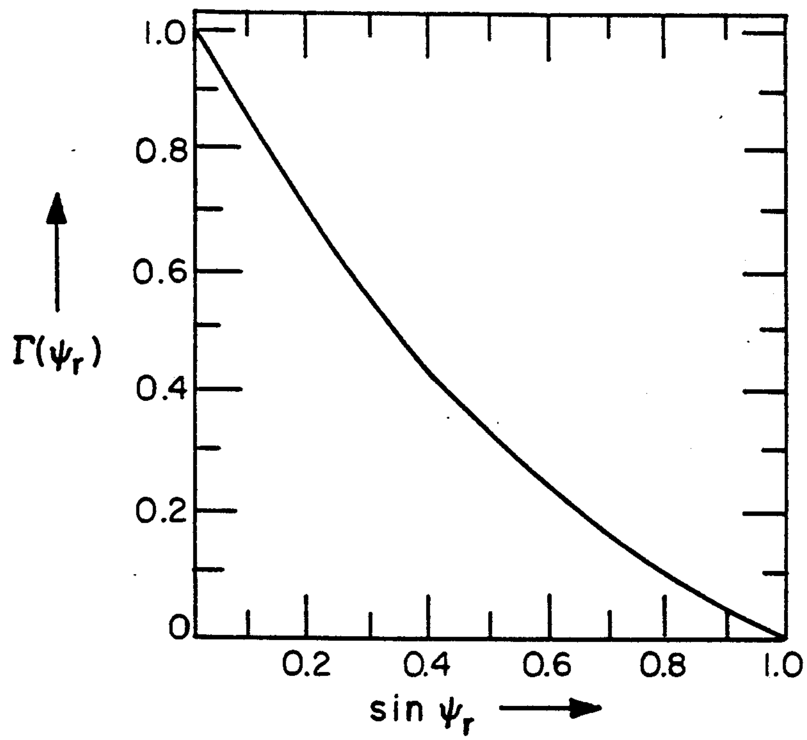

Fig. 3

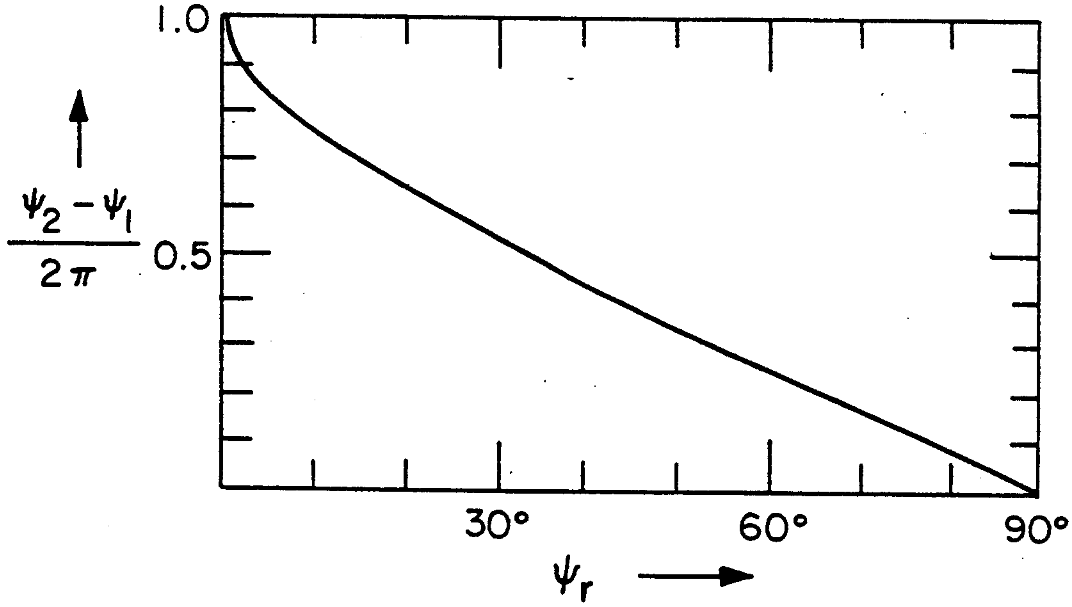

Fig. 4

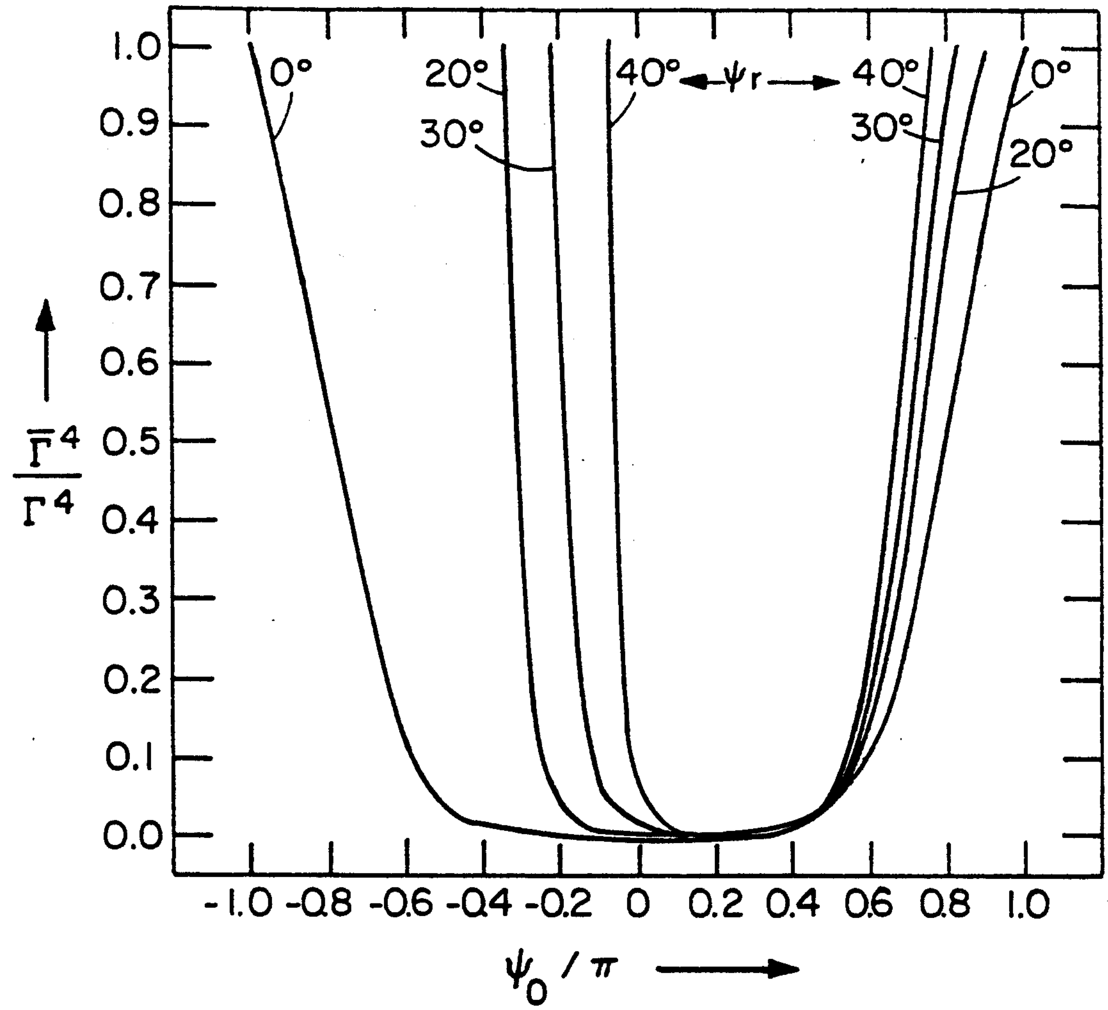
1.0
0.9
0.8
0.7
0.6
0.5
0.4
0.3
0.2
0.1
0.0
$\frac{\bar{\Gamma}^4}{\Gamma^4}$
0°
20°
30°
40°
ψ_r
40°
30°
0°
20°
-1.0 -0.8 -0.6 -0.4 -0.2 0 0.2 0.4 0.6 0.8 1.0
ψ_0/π

Fig. 5